

UDK 532.74; 622.785; 553.611

## Mineralogical Transformation and Microstructure of the Alluvials Clays

Bomeni Isaac Yannick<sup>1</sup>, Wouatong Armand Sylvain Ludovic<sup>1\*)</sup>, Ngapgue Francois<sup>2</sup>, Kamgang Kabeyene Véronique<sup>3</sup>, Fagel Nathalie<sup>4</sup>

<sup>1</sup>Department of Earth Sciences, University of Dschang, P.O. Box 67 Dschang Cameroon

<sup>2</sup>Department of Civil Engineering, Fotso Victor Institute of Technology, P.O. Box 134 Bandjoun Cameroon

<sup>3</sup>Department of Earth Science, Higher Teacher Training College, P.O. Box 47 Yaoundé Cameroon

<sup>4</sup>Department of Geology, University of Liege, 4000, Liege Belgium

---

### Abstract:

*Mineralogical transformations and microstructures during the firing alluvial clays from Monoun plain were studied. The firing of clays was carried out in the temperature range from 800 to 1150 °C. Minerals transformation was investigated by X-ray diffraction, polarize stereomicroscopy and scanning electron microscopy (SEM). In the raw materials, typical assemblages with quartz, kaolinite, goethite, anatase, hematite, gibbsite and feldspar were observed. Many neoformed mineral phases were identified with the reaction products including mullite, cristobalite, spinel, amorphous phase which occurred in the high temperature (1050 - 1150 °C) in the fired bricks. The quartz phenocrist with some microlites oxides embedded in few mesostasis glass have been illustrated at 950 °C by stereomicroscopy analysis. At 1150 °C, the vitreous matrix has embedded phenocrist of quartz and other relic minerals. The best temperature for fired alluvial clay brick was discovered between 1050-1150 °C.*

**Keywords:** *Thermal treatment; X-ray diffraction; Structure.*

---

## 1. Introduction

Clays are one of the most abundant natural mineral resources on earth [1]. They are used as raw materials in many industry fields such as ceramics, paper, paint, petroleum industry [2]. Ceramic clays are one of the most complicated ceramic systems because of the very complex relationship between the behaviour of minerals during the ceramic processing and the transformations during heating [3]. Nowadays, a major challenge is to predict the phase transformations in silicate ceramics, since complex relationships occur between the structural characteristics of the fired products and the physical properties [3]. In traditional ceramics, a series of transformation occurs during firing process which determine the final properties of the firing product [4, 5]. In case of fired bricks, the main factors involved in manufacturing are the type of raw materials, fabrication method, drying procedure and firing temperature. These factors will affect the quality of the final product [6]. During the sintering process in the brick manufacturing, stable initial raw materials transform into complex

---

\*) Corresponding author: [aslwouat@yahoo.com](mailto:aslwouat@yahoo.com)

compounds at high temperatures. New compounds are also formed due to chemical reactions that take place. Tite and Maniatis [7] have showed that vitrification of ceramic material is an important factor that influences the quality and physical properties of the end product such as strength and permeability. However, Livingston [8] suggested that the durability and strength of bricks are related to their microstructure and mineralogy. In Cameroon, numerous studies have been carried out to characterize and valorize industrial clays in ceramics. For instance, in the central region, Alluvial clay from Nanga Eboko and Ebebda can be used in firing bricks when sand is added to it [9]. Same characteristics are also observed on clays from Ngog-Lituba locality, where clayey materials are suitable for the production of earthenware at temperatures lower than 950 °C [10]. The hydromorphic clays from Yaoundé area have a high plastic index which makes it suitable for pottery and brick making [11], In the North-West region, Yongue et al. [12] show that alluvial clays from Ndop plain have varied colours like brown, grey and yellowish brown which can be used to produce roofing tiles, light weight blocks and hollow bricks at a temperature range from 900 to 1100 °C. In the North region, The Ngaye alluvial clastic clays could be used in the fabrication of bricks (commons and perforated) by the addition of fluxing agent to improve the mechanical performance of the ceramic products [13]. In the Far-North region, alluvial clays from Maroua are used in burnt brick when mixed with other clays, followed by the addition of a flexural agent [14]. In West region, the mineralogical content of alluvial clays from koutaba plain is, kaolinite (27-62 %), illite (2-13 %), smectite (1-25 %) and quartz (11-48 %). Those alluvial clays are inappropriate in ceramic products due to the high smectite contents (up to 20 %) and some treatments are needed like addition of quartz or sand before any ceramic application [15]. According to the preview works on Cameroonian clays, a few authors have survey the thermal behaviour of mineral during sintering. Therefore, this work is mainly devoted to mineralogical and microstructural transformation during firing bricks obtained from the Monoun alluvial clay.

## 2. Materials and Experimental Procedures

The raw alluvial clays used in this study were collected from Monoun plain during geological characterization of this clay deposit. A detailed mineralogical and physicochemical characterization as ceramic raw material has been done [16]. Fours samples labeled G, Y, B an M have been selected based on colours despite the similar mineralogical characterization of 133 clays samples from the Monoun plain alluvial clays. Their mineralogical and physicochemical compositions are reported in Table I-III.

**Tab. I** Mineralogical composition of raw samples.

Groups		Bulk Mineralogy (Powder)						Clay mineralogy ( $\theta < 2\mu\text{m}$ )			
Minerals	Quartz	Total Clay	K-feldspar	Anatase	Goethite	Hematite	Gibbsite	Kaolinite	Illite	Chlorite	
Corrective Factor of each mineral	11	20	4.30	0.73	7	3.33	0.95	0.7	1.00	0.34	
Authors of corrective factor	Cook et al. 1975	Boski et al. 1998	Cook et al. 1975				Thorez, 1976 in Fagel et al. 2003				
Samples code	G	27.3	55.9	11.2	1.1	3.5	0.6	0.4	84.5	10.3	5.2
	Y	17.3	60.1	6.0	1.3	13.1	2.0	0.2	76.3	19.4	4.3
	B	18.2	51.5	16.3	1.1	11.2	0.6	0.9	65.7	27.3	7.1
	Y	19.2	55.8	8.5	1.2	14.2	0.7	0.4	78.3	15.2	6.5

**Tab. II** Physical composition of alluvial clays from the Monoun plain.

Samples	G	Y	B	M
Clay ( $\Phi < 2\mu\text{m}$ )	73	59	26	51
Silt ( $20 > \Phi > 20\mu\text{m}$ )	23	23	44	22
Sand ( $2000 > \Phi > 20\mu\text{m}$ )	4	18	30	28
Liquidity limit (LI(%))	80	52	65	61
Plasticity limit (PI(%))	44	35	53	31
Plasticity index (PI)	36	17	12	31
Organic matter (Mo (%))	9	10	13	10

**Table III** Chemical composition of alluvial clays from the Monoun plain

Samples	G	Y	B	M
SiO <sub>2</sub>	56.5	44.9	52.3	51.6
TiO <sub>2</sub>	2.3	2.3	2.1	2.3
Al <sub>2</sub> O <sub>3</sub>	24.2	24.3	22.5	24.1
Fe <sub>2</sub> O <sub>3</sub>	3.1	10.4	4.4	6.0
MnO	0.0	0.0	0.0	0.0
MgO	0.3	0.3	0.3	0.2
CaO	0.1	0.1	0.2	0.2
Na <sub>2</sub> O	0.0	0.0	0.2	0.0
K <sub>2</sub> O	1.6	1.0	1.6	1.4
P <sub>2</sub> O <sub>5</sub>	0.2	0.2	0.2	0.2
LOI (%)	11.7	16.4	16.1	14.0

The samples were previously crushed in a porcelain mortar and sieved using a mesh of 1 mm and humidified at 5 % the under flow. The test specimen (80mm×40mm×10 mm) were made using a 10 kN hydraulic press, kept at room temperature for a day, then oven-dried 24 hours at 105 °C. The firing stage was carried out at a temperature range of 800 to 1150 °C in an oxidizing atmosphere at the Local Materials Promotion Authority (MIPROMALO) in Cameroon.

The crystalline phases in fired samples were identified by X-ray diffraction using a Bruker D8 Advance diffractometer (generator voltage: 40 kV; tube current: 30 mA; scan step size: 0.02°; time/step: 2 s) equipped with a copper anticathode ( $K\alpha=1.5418 \text{ \AA}$ ) in the laboratory AGES in Liege University, Belgium. The semi-quantitative analysis of crystalline phase was determined from the measured peak intensities multiplied by corrective factor [17].

The microstructure was performed on the flat polished surface to ensure the investigation on the real bulk structure of the products by using the Polarizing microscope and Scanning Electron Microscope (petrology laboratory and chemical laboratory in Liège University, Belgium).

### 3. Results and Discussion

#### 3.1. Study of the thermal behavior by XRD

The changes of the XRD diffractograms of alluvial clay samples from the Monoun plain with increasing temperature are illustrated in Figure 1 (a, b, c and d). Based on the results, quartz, feldspar, goethite, anatase, gibbsite, hematite, mullite, spinel and cristobalite

were detected. But kaolinite, which is presented in all raw samples (105 °C) disappeared completely at a temperature of 800 °C. From this temperature, the destruction of kaolinite coincided with the appearance of an amorphous product which can be metakaolinite [18, 19], according to the reaction (1):



In other, the XRD diffractogram show a decrease of the peak responses of clay minerals (4. 45Å) and indicate that, clay species have been transforming with the increase of temperature.

Above 950 °C, some remarkable changes have been noticed for the Y, B and M samples, contrarily to the sample G (Fig. 1 a) in which just a slight change was observed. The quartz peak intensity on sample G, Y, B and M begins to decrease due to the dissolution and to the conversion of a part of SiO<sub>2</sub> in cristobalite [20]. The feldspar and goethite peaks were slowly diminishing when sintered from 800 to 1150 °C (Fig. 1 a-d). This is due to the formation of the mullite phase [21], and hematite. At 1150 °C, a new phase of mullite, cristobalite, spinel and hematite have developed on Y, B and M samples (Fig. 1 b, c and d). Their peaks became sharp, showing a highly crystalline compound [22] while in G sample (Fig. 1 a), the intensity peaks of mullite, spinel and cristobalite remained weak. The new crystalline mineral phase non identified have been formed in G sample between 950 to 1150 °C and there are localised at reticular length of 8.40 Å and 6.50 Å.

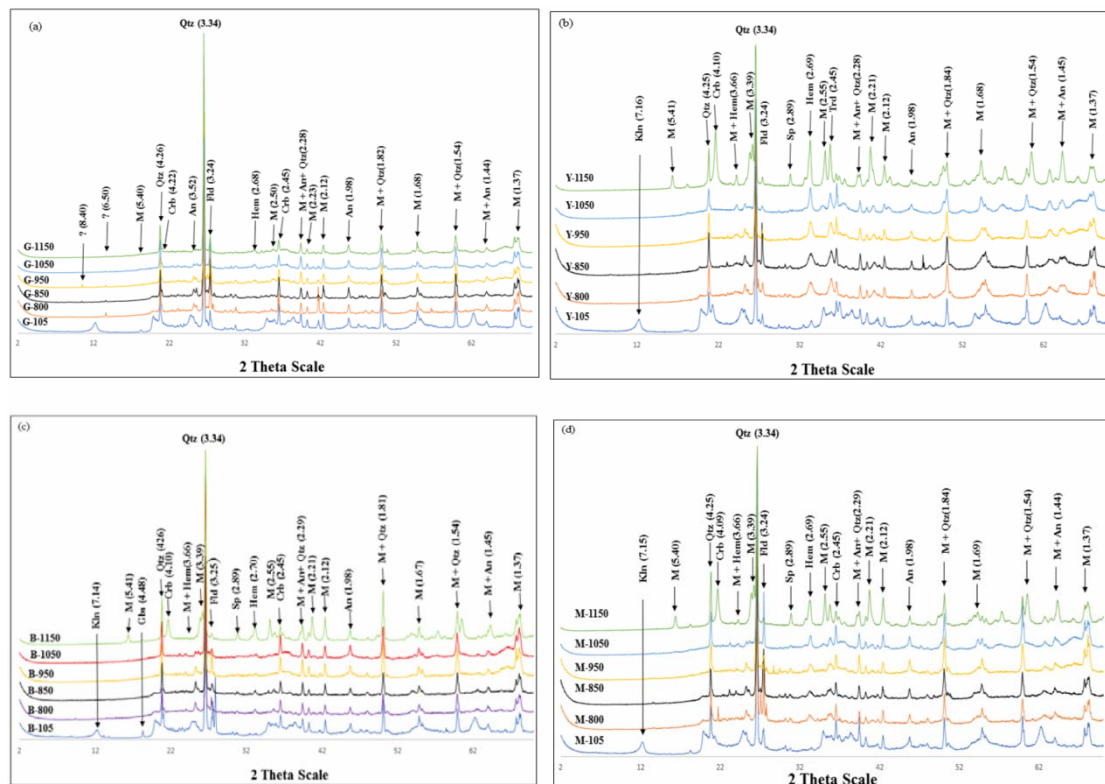


**Fig. 1.** XRD diffractograms of the alluvial clay fired at different temperatures: (a): Gray clay; (b): Yellow clay; (c): Black clay; (d): Mix color clay; An: Anatase; Crb: Cristobalite; Fld: Feldspar; Gbs: Gibbsite; Hem: Hematite; Kln: Kaolinite; M: Mullite; Sp: Spinel; Qtz: Quartz.

### 3.2. Quantitative data and phase transformations

The mineralogical transformations results are reported in Tables III to VI. Firstly, we remark on different tables (III, IV, V and VI), the proportion of mineral varying with the temperature of sintering and new minerals have appeared like mullite, cristobalite, spinel and hematite at the highest temperature (1150 °C) in all samples.

#### 3.2.1. Spinel phase

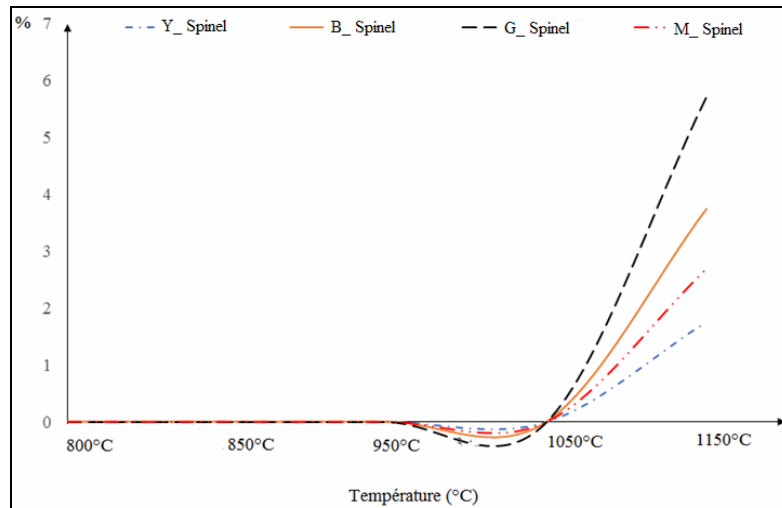


**Fig. 2.** Evolution of Spinel with the temperature of sintering.

Figure 2 resumed the evolution of spinel during sintering. The spinel phase showed a slant trend between 1050 to 1150 °C which explains the exponential increasing of spinel above 1050 °C. However, the high proportion of spinel is observed in the G clay sample (Table IV) with 5.72 % and weak amount (1.76 %) have been noticed in the Y clay sample (Table V).

**Tab. IV** Mineralogical transformations G clays during heating at different temperature.

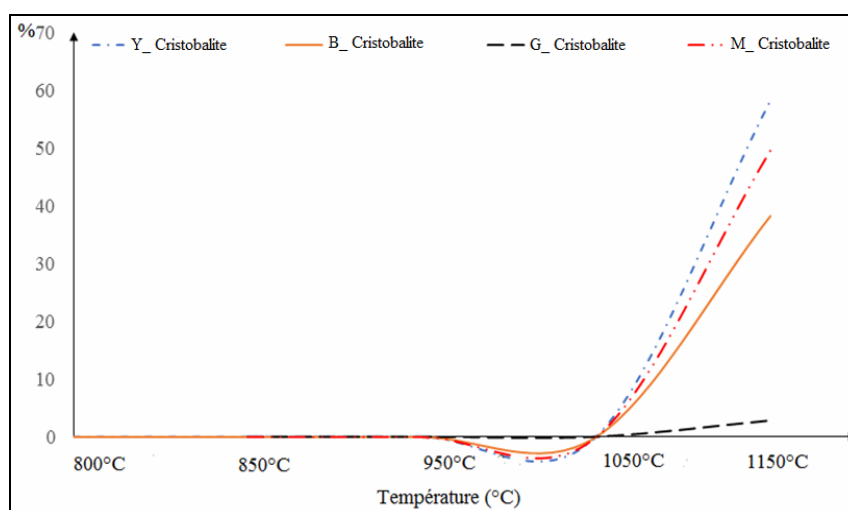
Gray Clay (G)	D (A°)	CF	800°	850°	950°	1050°	1150°
Total Clay	4.45	20	11.59	10.99	7.05	4.82	0.00
Mullite	3.39	2.8	0.00	0.00	0.00	0.00	1.98
Gibbsite	4.84	0.95	0.06	0.12	0.19	0.34	0.00
Spinel	2.88	2.1	0.00	0.00	0.00	0.00	5.72
Goethite	4.22	7	16.26	21.26	15.40	19.00	0.00
Hematite	3.66	3.33	0.55	0.46	1.88	2.97	2.65
Anatase	3.52	0.73	0.99	1.08	1.07	0.80	0.83
Quartz	3.34	1	23.63	32.43	39.18	37.04	64.08
Cristobalite	4.08	9	0.00	0.00	0.00	0.00	2.81
K-Feldspar	3.23	4.33	43.65	31.71	34.78	33.74	20.90
Plagioclase	2.85	2.8	3.27	1.96	0.45	1.29	1.02

**Tab. V** Mineralogical transformations Y clays during heating at different temperature.

Yellow clay (Y)	D (Å)	CF	800°C	850°C	950°C	1050°C	1150°C
Total Clay	4.45	20	18.74	16.08	10.79	9.17	0.00
Mullite	3.39	2.8	0.00	0.00	0.00	0.00	11.08
Gibbsite	4.84	0.95	0.14	0.17	0.24	0.55	0.00
Spinel	2.88	2.1	0.00	0.00	0.00	0.00	1.76
Goethite	4.22	7	16.24	17.46	28.32	36.66	0.00
Hematite	3.66	3.33	8.12	6.59	11.82	16.28	11.85
Anatase	3.52	0.73	1.76	1.44	1.94	1.37	0.38
Quartz	3.34	1	41.05	26.34	36.24	29.31	13.49
Cristobalite	4.08	9	0.00	0.00	0.00	0.00	58.12
K-feldspar	3.23	4.33	11.58	31.44	10.35	6.29	3.11
Plagioclase	2.85	2.8	2.36	0.48	0.30	0.37	0.21

### 3.2.2. Cristobalite phase

Cristobalite is a high temperature polymorph of silica which is observed through the  $d_{101}$  diffraction peak at 4.08 Å. The proportional increase with sintering temperature above 1050 °C in all samples (Fig. 3). The increasing amount is generally linked to the crystallization of amorphous silica, which is derived from the transformation of metakaolinite into mullite [23]. Then, the Y sample gives a high value of cristobalite (58.12 %) on sintering ranging from 1050 to 1150 °C (Table V). On contrary, the low value of cristobalite (2.81 %) is observed in the G sample (Table IV). This contrast can be explained by the lack of fluxing agent in G sample.

**Fig. 3.** Evolution of cristobalite with the temperature of sintering.

### 3.2.3. Mullite phase

The mullite is an aluminosilicate compound that is used for conventional and advanced ceramic applications due to low density, low thermal conductivity, low thermal

expansion, low dielectric constant, excellent mechanical properties at high temperature [24]. In our test specimen, primary mullite started neoformation at 1050 °C and increased gradually with temperature (Fig. 4). Therefore, high proportions of mullite were observed in the M sample (13.72 %) (Table VI) and lower values have been observed in the G sample (1.98 %) (Table IV). The high value of mullite in the M sample is due to the melting phase and impurities like Fe<sub>2</sub>O<sub>3</sub> [25]. The mineralogy shows that the M sample contains 14.2 % of goethite (Table I) which confirms the above hypothesis.

**Tab. VI** Mineralogical transformations B clays during heating at different temperature.

Black clay (B)	D (Å)	CF	800°C	850°C	950°C	1050°C	1150°C
Total Clay	4.45	20	49.33	21.65	7.24	5.52	0.00
Mullite	3.39	2.8	0.00	0.00	0.00	0.00	13.52
Gibbsite	4.84	0.95	0.14	0.19	0.17	0.27	0.00
Spinel	2.88	2.1	0.00	0.00	0.00	0.00	3.74
Goethite	4.22	7	12.60	20.07	20.58	30.17	0.00
Hematite	3.66	3.33	2.08	3.23	1.34	2.31	6.42
Anatase	3.52	0.73	1.25	2.51	1.57	1.11	0.32
Quartz	3.34	1	22.60	40.83	44.08	50.96	33.27
Cristobalite	4.08	9	0.00	0.00	0.00	0.00	38.17
K-feldspar	3.23	4.33	11.22	10.63	22.65	9.10	4.20
Plagioclase	2.85	2.8	0.78	0.89	2.38	0.56	0.36

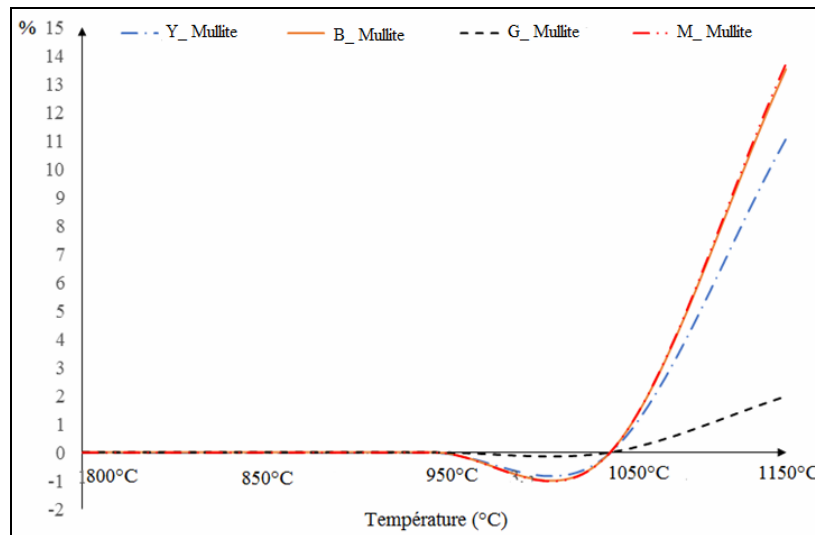


**Fig. 4.** Evolution of mullite with the temperature of sintering.

### 3.2.4. Goethite phase

The goethite is a thermal conductor mineral or fluxing agent during ceramic processing. Its evolution during firing is summarized in Figure 5. In all the fired samples, the maximum value obtained reached at 1050 °C and gradually disappeared until 1150 °C. At 1050 °C, the high amount of goethite during sintering have been show in Y sample (36.66 %) (Table III). The decreasing amount of goethite contrast with increase amount of hematite

except Y sample. This observation confirms that the fluxing agent played a role during sintering and transformation of goethite to hematite according to [26] by the reaction (2):

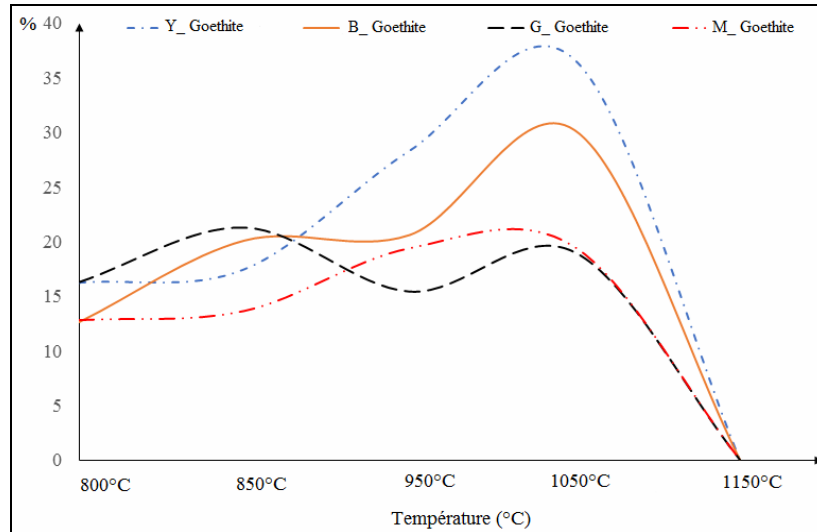


**Fig. 5.** Evolution of goethite with the temperature of sintering.

### 3.2.5. Hematite phase

Hematite is an unstable mineral in ambient temperature [27] and is rarely observed. The Fig. 6 illustrated the variation of hematite phase with the temperature. We can observe that, hematite ( $\text{Fe}_2\text{O}_3$ ) begins to crystallize at 850 °C in all samples and continues to increase until 1150 °C (Fig. 6). This neoformation of hematite with increase in temperature have been reported by [28]. However, in the Y sample, the hematite phase decrease particularly at 1050 °C. This is due to the fusion of some minerals at low temperature which got imbedded in the vitreous matrix.

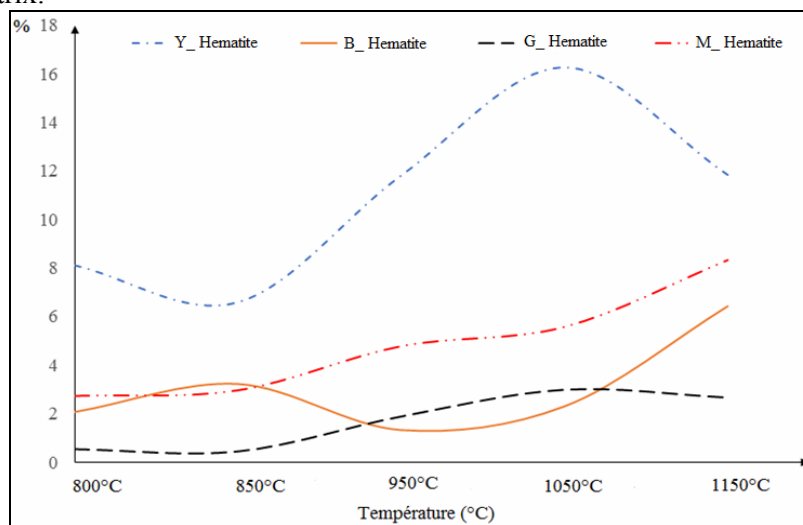


**Fig. 6.** Evolution of hematite with the temperature of sintering.

### 3.2.6. Feldspar phase

The feldspar phase varies significantly with the increasing temperature and presented a sinusoidal trend (Fig. 7). We observed two bearing from M sample at 850 and 1050 °C. In other, one bearing has also seemed on the Y, B sample respectively at 850 and 950 °C (Tab. VII). After the range, the proportion of feldspar decreases. This behaviour follows the melting point of mineral and the appearance of the vitreous phase which fills the pores between the grains during firing [29].

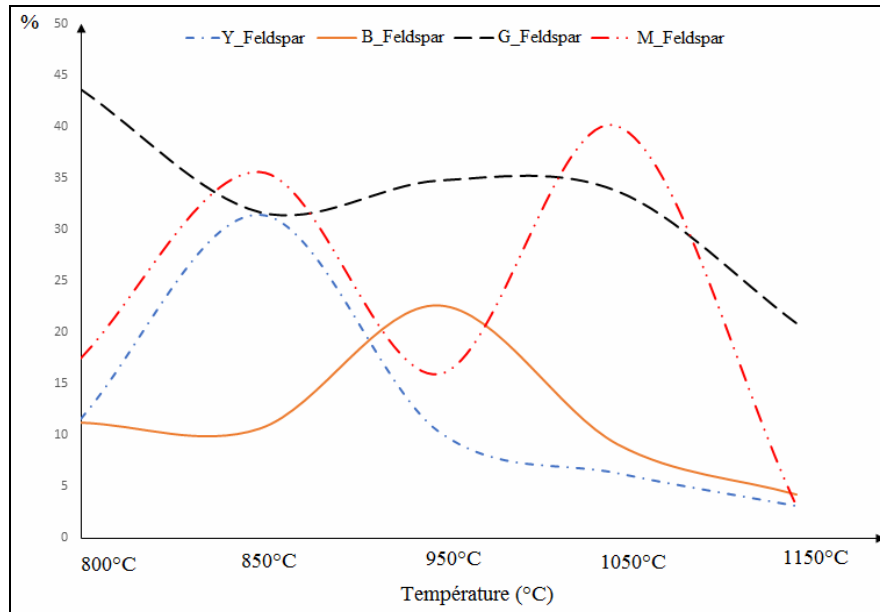


Fig. 7. Evolution of Feldspar with the temperature of sintering.

Tab. VII Mineralogical transformations M clays during heating at different temperature.

MIX COLOR CLAY (M)	D (Å)	FC	800 °C	850 °C	950 °C	1050 °C	1150 °C
Total Clay	4.45	20	14.60	16.20	7.52	2.67	0.00
Mullite	3.39	2.8	0.00	0.00	0.00	0.00	13.72
Gibbsite	4.84	0.95	0.10	0.19	0.31	0.27	0.00
Spinel	2.88	2.1	0.00	0.00	0.00	0.00	2.69
Goethite	4.22	7	12.80	13.64	19.38	19.50	0.00
Hematite	3.66	3.33	2.75	2.98	4.79	5.58	8.32
Anatase	3.52	0.73	1.08	1.33	1.54	0.73	0.33
Quartz	3.34	1	32.05	29.47	47.67	30.83	22.02
Cristobalite	4.08	9	0.00	0.00	0.00	0.00	49.57
K-feldspar	3.23	4.33	17.47	35.56	15.93	40.01	3.13
Plagioclase	2.85	2.8	19.14	0.62	2.85	0.41	0.22

### 3.2.7. Plagioclase phase

The proportion of plagioclase in all samples which played the role of fluxing agent during sintering has been summarized in Fig. 8. This Fig. 8 shows the decrease of plagioclase with increase in temperature. Furthermore, one particularity is noticed on M sample, being the exponential decrease between 800 to 850 °C (19.14 % - 0.62 %) thereafter, increasing slightly between 850 to 950 °C and disappearing at 1150 °C.

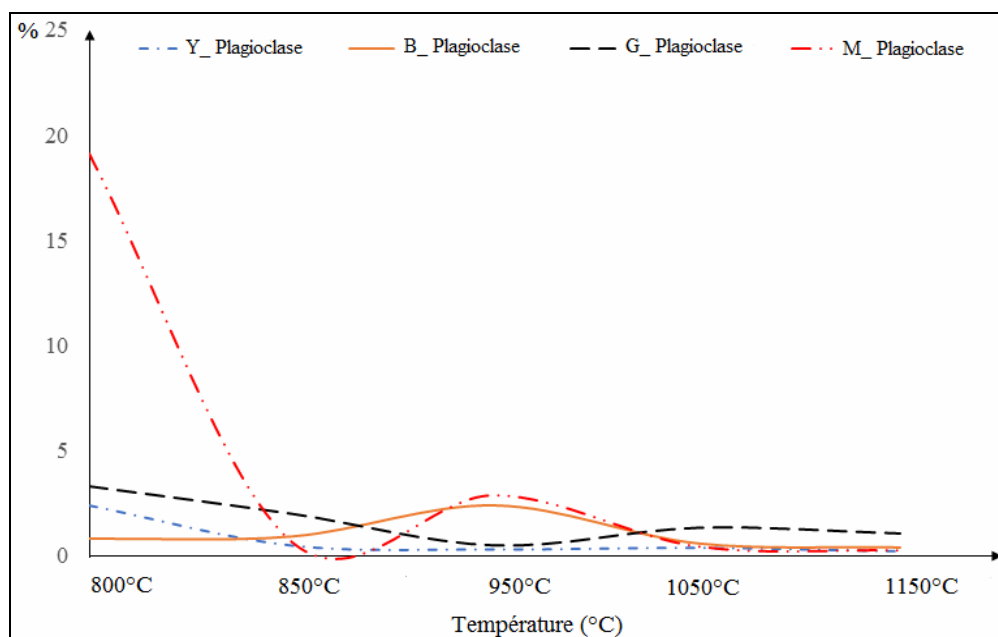


**Fig. 8.** Evolution of plagioclase with the temperature of sintering.

### 3.3. Microstructure of firing brick

#### 3.3.1. Microstructure in Polarize microscope

The result obtained from the analysis from polarizing stereo microscopy are show in Fig. 9. Under the polarize stereomicroscope at 950 °C, the firing facies (G, Y, B and M) have shown a microgranular texture characterized by quartz phenocrist and some microlites oxides embedded in the few microlitic glass mesostasis. This behaviour is consistent with that found by [30], who showed that the brick structure formed at lower temperatures (840-960 °C) remained essentially the same until temperatures of over 1080 °C are reached. However, the matrix of the fired specimens has different appearance from other due to the nucleate development of hematite [1] where it can be recognized as few small crystals dispersed in a uniform red Fe-rich surface (Fig. 9). At 1150 °C, the solid state sintering become very significant and characterized by vitreous matrix in which is embedded phenocrist of quartz and neoformed minerals. Moreover, all sintering specimen present numerous open pore which define many texture like entangle in B specimen; porphyritic grainy in the M specimen and micrograiny in the G and Y specimens.

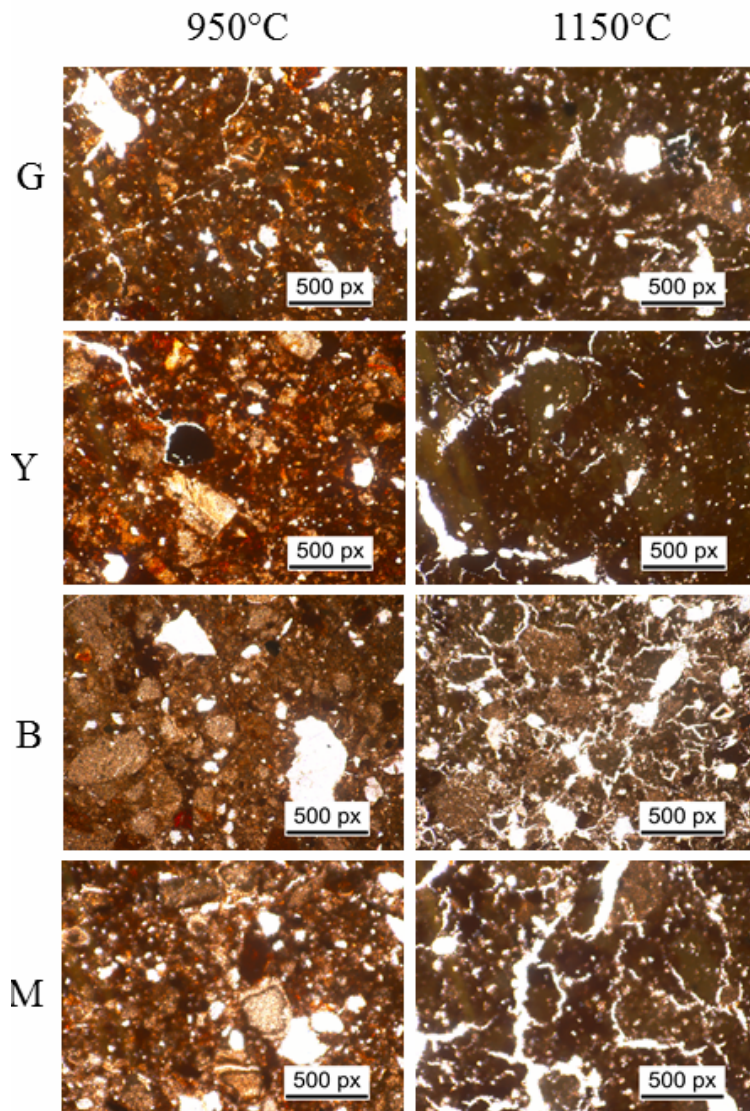


**Fig. 9.** Scanning electron micrographs of polished surface of G, Y, B, M samples firing at 950 and 1150 °C: H: hematite, Q: quartz, P: pore, NM: neoformed mineral, V: vitreous matter.

### 3.3.2 Scanning Electron Microstructure

Fig. 10 shows the microstructure with EDS analysis of sintering specimen G, Y and M at 950 and 1150 °C. the scanning view show a dominant vitrification at 1150 °C and numerous pores which tend to have varied sizes and forms. The varied sizes of pores may be generated by the diffusive gas flow emanations (water and carbon dioxide) upon firing specially by the action of transforming clays [30, 31]. This high porosity of the ceramics implies the presence of closed and open pores, which are important for the evaluation of the brick products properties [32]. The elemental mapping by EDS revealed that silicium, aluminium and iron are present in higher concentration close to the surface at 1150 °C. This remark is in conformity with the new mineral identified by XRD analysis like mullite, cristobalite and spinel which results from the combination of different ions during the melt process.

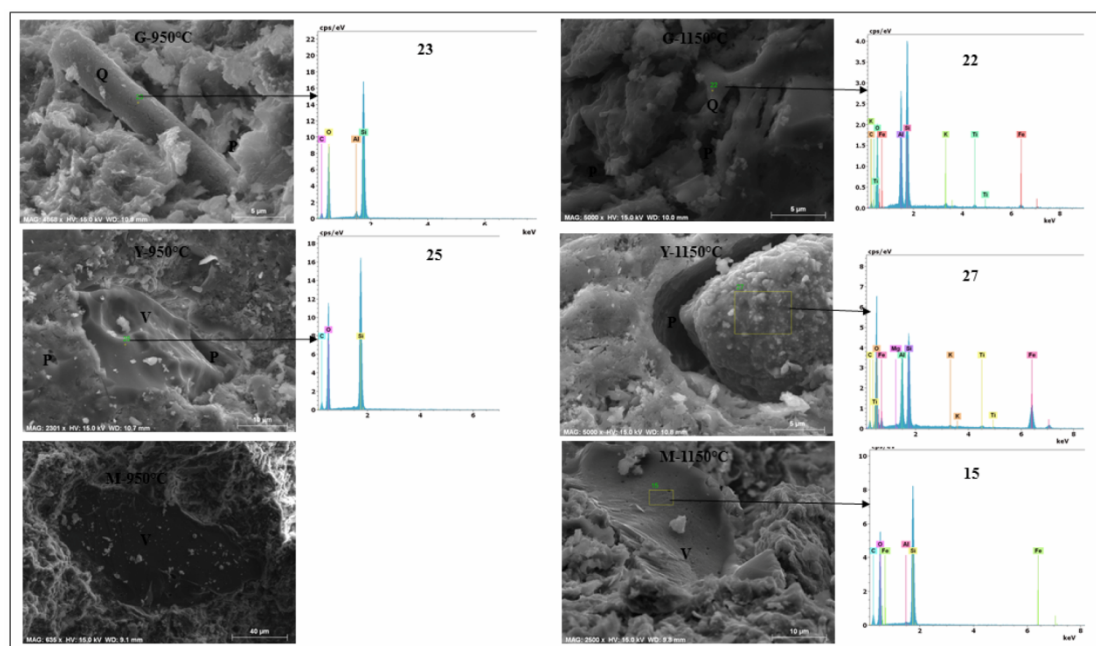


**Fig. 10.** Scanning Electron Microscope and EDS of firing alluvial clay at 950 and 1150 °C  
Q: Quartz, P: pore, V: vitreous matter, NM: neofomed mineral.

#### 4. Conclusion

The study of four different colours of alluvial clays (G, Y, B and M) from Monoun plain has indicated similar mineralogical composition. The major phases present in the raw clays are quartz, kaolinite, illite, chlorite, feldspar, anatase, goethite, hematite and gibbsite. Several mineral phases were identified in the fired clays, with the reaction products including mullite, cristobalite, spinel, residual quartz, hematite and an amorphous phase (glass generated by melting of feldspars and clays) in the fired clays. The evolutionary quantification of previous minerals has shown a decrease with the increase sintering temperature. However, the new phases of minerals can be identified until 1050 °C and increase gradually with the temperature. The stereomicroscopy analysis at 950 °C have shown quartz phenocryst with some microlites oxides embedded in few mesostasis glass which define the microgranular texture. In others, at 1150 °C we observed a vitreous matrix in which is embedded phenocryst of quartz and other relic minerals. This observation has been confirmed by electronic microscopy, that the firing has a positive influence on the neofomed mineral and microstructure of brick. The best firing temperature for the alluvial clay brick was observed between 1050-1150 °C.

#### 5. References

1. O. M. Castellanos, C. A. Ríos, M. A. Ramos, E. V. Plaza, *Boletín de Geología*. 34 (2012) 43.
2. L. L. Y. Chang *Industrial mineralogy: Materials, processes, and uses*. Prentice Hall, New Jersey, (2002) 472.
3. F. Pardo, S. Meseguer, M. M. Jordán, T. Sanfeliu, I. González, *Appl. Clay Sci.* 51 (2010) 147.

4. F. González-García, V. Romero-Acosta, G. García-Ramos, M. González Rodríguez, *Appl. Clay Sci.*, 5 (1990) 361.
5. M. M. Jordán, T. Sanfeliu, C. De la Fuente, *Appl. Clay Sci.*, 20 (2001) 87.
6. I. Johari, S. Said, B. Hisham, A. Bakar, Z. A. Ahmad, *Sci. Sinter.*, 42 (2010) 245.
7. M. S. Tite, Y. Maniatis, *Trans. British. Ceram Soc.*, 74 (1975) 229.
8. R. A. Livingston, P. E. Stutzman, I. Schumann, Quantitative X-Ray Diffraction Analysis of Handmolded Brick. In: *Foam Conservation of Historic Brick Structures - Chapter 11* (Eds. Shafesburg, U.K., Baer, N.S., Fritz, S., and Livingston, R.A.), Donhead Publishing Ltd, 1998 pp. 105-116.
9. A. Nzeukou, N. Fagel, A. Njoya, V. Kamgang, R. Medjo, U. Chinje, *Appl Clay Sci.*, 83-84 (2013) 238.
10. P. D. Ndjigui, J. A. Mbey, A. Nzeukou Nzeugang, *J. Build Eng.*, 5 (2016) 151.
11. G. F. Ngon Ngon, R. Yongue Fouateu, D. L. Bitom, P. Bilong, *J Afri Earth Sci* 55., (2009) 69.
12. R. Yongue Fouateu, F. Ndimukonga, A. Njoya, *J. Asian Ceram Soc.*, 4 (2016) 299.
13. F. Djenabou Soureiyatou, P. D. Ndjigui, J. A. Mbey, *J. Asian Ceram Soc.*, 3 (2014) 50.
14. D. Tsozué, A. Nzeukou Nzeugang, J. R Mache, S. Loweh, N. Fagel, *J Buil Eng.*, 11 (2017) 17.
15. A. NKalih Mefire, *Cartographie et propriétés physico-chimiques des argiles de Fouban (Ouest-Cameroun. Thèse de doctorat en cotutelle Université de Liège Belgique et Université de Yaoundé I Cameroun, (2016) 167.*
16. I. Y. Bomeni, A. S. L. Wouatong, F. Ngapgue, V. Kamgang Kabeyene, N. Fagel, *J. Clay Sci. Japan.*, 22 (2018) 29.
17. H. E. Cook, P. D. Johnson, J. C. Matti, I. Zemmels *Methods of sample preparation and X-ray diffraction in X-ray mineralogy laboratory. Deep Sea Drilling Project, University of California, Riverside. Contribution, 74-5 (1975) 999-1007.*
18. G. Kakali, T. Perraki, S. Tsivilis, E. Badogiannis, *Appl. Clay Sci.*, 20 (2001) 73.
19. C. Y. Chen, C. S. Lan, W. H. Tuan, *Ceram. Int.*, 26 (2000) 715.
20. A. Bennour, S. Mahmoudi, E. Srasra S. Boussen, N. Htira, *Appl. Clay Sci.*, 115 (2015) 30.
21. M. M. Jordan, M. A. Montero, S. Meseguer, T. Sanfeliu, *Appl. Clay Sci.*, 42 (2008) 266.
22. P. Chindraprasirt, K. Pimraksa, *Powder Technol.*, 182 (2008) 33.
23. E. Kamseu, C. Leonelli, D. N. Boccaccini, P. Veronesi, P. Miselli, G. Pellacani, U. C. Melo, *Ceram Int.*, 33 (2007) 851.
24. E. Tutić, M. Jovanović, A. Mujkanović, *Sci Sint.*, 48 (2016) 247-257.
25. F. Pardo, S. Meseguer, M. M. Jordán, T. Sanfeliu, I. González, *Appl Clay Sci.*, 51 (2010) 147.
26. G. Brown, G. W. Brindley, *Mineral. Soc. London.* (1984) 495.
27. G. F. Ngon Ngon, R. Yongue Fouateu, D. L. Bitom, P. Bilong, *Afr. Earth Sci.*, 55 (2009) 69.
28. E. Escalera, R. Tegman, M. L. Marta-Lena Antti , M. Odén, *Appl. Clay Sci.*, 101 (2014) 100.
29. E. Lambercy, *Les matières premières céramiques et leurs transformations par le feu. Granit1. Des dossiers argiles (1993) 509.*
30. A. C. S. Alcântara, M. S. S. Beltrão, H. A. Oliveira, I. F. Gimenez, L. S. Barreto, *Clay Sci.*, 39 (2007) 160.
31. G. Cultrone, E. Sebastián, K. Elert, M. J. De la Torre, O. Cazalla, C. Rodríguez-Navarro, *J. Eur. Ceram. Soc.*, 24 (2004) 547.
32. M. Vlasova, P. A Márquez Aguilar, V. González Molina, A. Trujillo Estrada, M. Kakazey, *Sci. Sint.*, 50 (3) (2018) 275-289.

---

**Садржај:** Проучаване су минеролошке трансформације и микроструктуре током спаљивања алувијалних глина са Моноун равни. Глине су печене у температурском интервалу од 800 до 1150°C. Трансформације минерала су испитиване рендгенском дифракцијом, поларизованом стереомикроскопијом и скенирајућом електронском микроскопијом. У почетним материјалима, уочена је типична структура која садржи кварц, каолинит, гетит, анатас, хематит, гипсит и фелдспар. Многе новоформиране фазе су детектоване на високим температурама, од 1050 до 1150°C, мулит, кристобалит, спинел и аморфне фазе. Стереомикроскопском анализом је представљен кварц на 950°C. Откривено је да је оптималан температурски интервал за печење цигли од алувијалне глине између 1050-1150 °C.

**Кључне речи:** термички третман, рендгенска дифракција, структура.

---

© 2018 Authors. Published by the International Institute for the Science of Sintering. This article is an open access article distributed under the terms and conditions of the Creative Commons — Attribution 4.0 International license (<https://creativecommons.org/licenses/by/4.0/>).

